Functional connectivity favors hyperactivity leading to synapse loss in amyloidosis

Oliver J. L'Esperance, Josh McGhee, Garett Davidson, Adam Steven Smith, Jaichandar Subramanian*

Department of Pharmacology and Toxicology, School of Pharmacy, University of Kansas, Lawrence, KS 66045, USA

Running title: Functional and synaptic connectivity in amyloidosis

* Corresponding author address: Department of Pharmacology and Toxicology, 1251 Wescoe Hall Drive, Malott Hall Room 5060, University of Kansas, Lawrence, KS 66045

Phone: 785-864-3110; Email: jaichandar@ku.edu

Author contributions: O.J.L, A.S.S. and J.S designed the experiments and analysis. O.J.L, J.M, and G.D performed the experiments and analyzed the data. O.J.L and J.S wrote the manuscript. J.S. supervised the research.

ABSTRACT

Hyperactivity is observed in early Alzheimer's disease (AD) in multiple brain regions, including the visual cortex. We recently found that the postsynaptic structures favor visual cortex hyperactivity, which disrupts functional connectivity and leads to visual recognition memory deficits in a mouse AD model. It is unclear whether presynaptic structures also favor hyperactivity and whether hyperactivity depends on the target or source of presynaptic terminals. In addition, it is not well understood whether the functional connectivity of brain regions under nonpathological conditions predicts their hyperactivity in amyloid pathology. We used c-Fos immunolabeling under resting state conditions to map brain-wide neural activity and performed network analysis. We also quantified excitatory and inhibitory presynaptic terminals in hyperactive and non-hyperactive brain regions.We found that hyperactivity in the visual network originates in the cortex, and brain regions highly connected to the primary visual cortex in nonpathological conditions tend to be hyperactive in amyloid pathology. Immunolabeling presynaptic terminals from subcortical and cortical neurons show that the source rather than the target brain regions determine the vulnerability of synapses. Furthermore, we observed a reduction in presynaptic structures selectively in the hyperactive region, indicating presynaptic changes are unfavorable to hyperactivity. Brain regions with higher functional connectivity under nonpathological conditions are vulnerable to hyperactivity in amyloid pathology. Furthermore, presynapse loss may serve as an adaptation to maintain neuronal activity homeostasis.

INTRODUCTION

Neuronal hyperactivity occurs early in some Alzheimer's disease (AD) patients and mouse models of amyloidosis[1-21]. Multiple cellular and synaptic mechanisms, including structural synaptic changes, increased excitation, reduced inhibition, altered intracellular calcium levels or extracellular glutamate levels are associated with hyperactivity[1, 2, 6-8, 10, 11, 13-16, 22-44]. Hyperactivity elicited by disruption of any of these factors may occur independently in different brain regions. Alternatively, hyperactivity originating in a brain region may spread globally due to properties of network connectivity. Consistently, the highly connected default mode network has been found to be hyperactive in AD patients[4, 45-50]. Hyperconnectivity and hyperactivity may influence each other under pathological states, but the extent to which functional connectedness under nonpathological conditions predispose circuits to hyperactivity in amyloidosis is unclear.

Neuronal hyperactivity is observed in circuits beyond the default mode network and the hippocampus[1, 21, 23, 51-55]. The visual cortex is one of the understudied brain regions in the context of AD due to the absence of gross structural deficits in this brain region until very late stages[56-59]. However, in some patients the visual cortex is affected early in the disease progression, and these patients exhibit profound visuospatial defects[60-72]. Neuronal hyperactivity and is also observed in the visual cortex of AD patients[52, 54, 60, 73]. Likewise, many mouse models of AD exhibit structural and functional deficits in the visual cortex[1, 2, 23, 51, 53, 74-81]. We recently found that visual cortex hyperactivity disrupts local functional connectivity and impairs visual recognition memory in a mouse model of amyloidosis[1]. Interestingly, the changes to excitatory and inhibitory postsynaptic densities favored hyperactivity[1]. However, it is unclear whether presynaptic structures are differentially

influenced by hyperactivity. Since hyperactive regions progress to a hypoactive state in AD[22, 46, 82-87], increased hyperactivity favored by postsynaptic structures could be compensated by loss of presynaptic structures, leading to eventual hypoactivity.

Using visual network as a model, we test whether functional connectedness under nonpathological conditions favors hyperactivity, which in turn lead to the loss of presynaptic terminals in a mouse model of amyloidosis (J20 line) at a pre-plaque stage. Using immediate early gene expression-based network mapping, we found that functional connectedness under nonpathological conditions is a significant predictor of network hyperactivity. We additionally found that hyperactivity is associated with localized loss of specific excitatory presynaptic markers, indicating that presynaptic changes oppose hyperactivity. Interestingly, the loss of presynaptic terminals is not dependent on hyperactivity in their target brain region, indicating that cell-intrinsic properties may influence synapse loss.

MATERIALS AND METHODS

ANIMALS

All animal procedures are approved by the University of Kansas Institute of Animal Use and Care Committee and meet the NIH guidelines for the use and care of vertebrate animals. PDGF-hAPP transgenic mice (J20 line; Gladstone) were maintained as heterozygotes for the hAPP transgene by breeding heterozygous J20 male mice with WT female mice. A maximum of five mice were housed in a standard cage. Mice were housed on a 12h-light/12h-dark cycle.

TISSUE PREPARATION AND IMMUNOHISTOCHEMISTRY

Mouse cages were brought to the surgical suite at least five hours before brain extractions to avoid capturing c-Fos expression elicited by movement or contextual novelty. 3.5-6-month-old (synapse immunohistochemistry) or 5-6-month-old (c-Fos immunohistochemistry) J20-hAPP

and WT littermate mice were deeply anesthetized by intraperitoneal injection of 2% avertin in phosphate-buffered saline (PBS), pH 7.4 and transcardially perfused with cold PBS followed by 4% paraformaldehyde. The brains were extracted and post-fixed in 4% PFA overnight at 4°C, followed by storage in PBS. For 40µm slicing, the brains were embedded in 4% oxidized agarose as previously described[88] to limit artifacts during sectioning and sliced on a vibratome (Leica VT1000 S). For 20µm slicing, brains were cryoprotected overnight at 4°C in 15% (w/v) and then in 30% (w/v) sucrose in phosphate buffer (PB). The brains were sectioned coronally on a microtome (Leica SM 2010R) and collected in PBS with sodium azide (0.02%).

24 evenly spaced 40µm slices from each brain spanning the posterior midbrain to the anterior olfactory bulb were fluorescently immunolabeled for c-Fos, and 3 evenly spaced 20-40µm slices spanning the VIS, AUD, and LGD (1-2 slices for each region per mouse) were fluorescently immunolabeled for VGAT, VGluT1, and VGluT2. Sections were permeabilized for 2h at room temperature in a 1% TritonX-100 and 10% normal goat serum (NGS) solution in PBS followed by incubation with rabbit anti-c-Fos (1:1000, CST) or rabbit anti-VGAT (1:1000, Synaptic Systems), mouse anti-VGluT1 (1:2000, Sigma), and guinea pig anti-VGluT2 (1:1000, Sigma) in a PBS solution containing 0.1% TritonX-100 and 5% NGS overnight at 4°C. Sections were then washed 3X with PBS and incubated with Alexa 555-conjugated goat anti-rabbit antibody (1:2000; Fisher) for c-Fos immunohistochemistry or Alexa 488 conjugated goat anti-rabbit antibody (1:2000, Fisher), Alexa 555-conjugated goat anti-mouse antibody (1:2000, Fisher), and Alexa 647-conjugated goat anti-guinea pig antibody (1:2000, Fisher) for two hours in a PBS solution containing 0.1% TritonX-100 and 5% NGS at room temperature, followed by three washes with PBS before mounting on glass slides. Slices were imaged using an ImageXpress Pico automated imaging system (Molecular Devices, San Jose, CA) with a 10x

objective for c-Fos acquisition (Leica HC PL FLUOTAR 10x/0.32) and a 63x objective for presynaptic termini acquisition (Leica HC PL FLUOTAR 63x/0.70 CORR).

ANALYSIS

Slice registration, cell/synapse detection, and brain region area measurements were performed using NeuroInfo software (MBF Bioscience, Williston, VT). 12-bit slice images were first mapped in 3D to the Allen CCF v3 to allow automated cell/synapse detection and area measurement by region. A total of 31 regions covering the entire cerebral cortex, cerebral nuclei, interbrain, and midbrain, and 17 subregions of the visual network were mapped for analysis. Bright circular objects against a darker background were automatically detected using a scale-space analysis of the response to Laplacian of Gaussian (LoG) within the expected range of labeled cell body or synaptic puncta diameters as described[89]. Briefly, cells/synapses were filtered out from all identified objects with a user-defined threshold based on the strength of the LoG response within an expected range of cell body diameters. The LOG threshold value was set at LoG threshold = 55 for cell bodies and 101 for all synapses (range 0-255). Only objects above this LoG strength threshold were included in the analysis to minimize false positives. All regions in both hemispheres of the 24 brain-wide slices were analyzed for c-Fos^{+} cell detection. For synapse quantification, 1-2 ~230 x 900µm columns per mouse spanning all layers of the VIS or AUD were analyzed, and 1-2 ~230 x 375µm columns per mouse spanning the ventral to dorsal LGD were analyzed. Automatically identified cells and synapses were manually proofread, and remaining false positive identifications were removed before analysis. Cell/synapse density for each mouse was calculated by dividing the total number of cells or synapses per region by the area per region across all slices for each brain (24 slices for c-Fos, 2-3 slices for synapses). Localized areas containing artifacts were excluded from analysis. 8 WT (6 males, 2 females) and

9 hAPP mice (4 males, 5 females) were used for c-Fos$^+$ cell density analysis, and 14 WT (9 males, 7 females) and 12 hAPP mice (6 males, 6 females) were used for presynaptic density analysis. GePhi (Association GePhi, London, England) was used to produce circular network graphs and network statistics. Representative images were generated in FIJI (NIH, Bethesda, MD), and all other figures and statistical tests were produced in GraphPad Prism (GraphPad Software, San Diego, CA).

RESULTS

VISUAL NETWORK HYPERACTIVITY IS LOCALIZED TO CORTICAL REGIONS IN HAPP MICE

We recently found increased c-Fos$^+$ cell density in the primary visual cortex in ~5-month-old hAPP-overexpressing mice compared to control siblings, indicating hyperactivity in pre-plaque stage amyloidosis[1]. Primary visual cortex hyperactivity may arise due to hyperactivity in subcortical structures that project to the visual cortex. In turn, the primary visual cortex may influence hyperactivity in other brain regions through their functional connections. Therefore, we characterized c-Fos$^+$ cell density across 24 evenly spaced slices spanning the brain in hAPP mice and WT littermate controls (Figure 1A-C., see Supplementary Table 1 for region abbreviations). To test whether subcortical brain regions that project to visual cortex are hyperactive, we compared c-Fos$^+$ cell density in the lateral geniculate nuclei and superior colliculus and found no significant difference between hAPP and WT mice (Figure 1D, left). However, c-Fos$^+$ cell density was significantly increased in the primary visual cortex. Within the primary visual cortex, we compared c-Fos$^+$ cell density between hAPP and WT mice in different layers to test whether hyperactivity originates in specific layers. We found that all layers, including layer 4, which receives subcortical inputs, show hyperactivity (Figure 1D, right). We next tested whether

hyperactivity is limited to the primary visual cortex or spread out in the rest of the higher visual cortical areas. We found that c-Fos$^+$ cell density was significantly higher in all higher order visual cortical areas in hAPP mice (Figure 1D, right). These results indicate that visual network hyperactivity originates in cortex in early-stage amyloidosis.

HYPERACTIVITY-ASSOCIATED SYNAPSE LOSS DEPENDS ON THE SOURCE OF PRESYNAPTIC INPUTS

Increases and decreases in synaptic density are likely to enhance or lower regional neuronal activity, respectively. We first tested whether synaptic density differs between hAPP and control mice depending on the hyperactivity state of a brain region. We performed immunolabeling for excitatory presynaptic proteins of cortical and thalamic neurons (VGluT1 and VGluT2, respectively) and inhibitory presynaptic proteins (VGAT) in two visual network regions: the primary visual cortex (hyperactive) and the dorsal lateral geniculate nucleus (non-hyperactive) (Figure 2A). We found a significant reduction in VGluT1, but not VGluT2 or VGAT densities in hAPP mice in the primary visual cortex and a similar trend of reduction in the dorsal lateral geniculate nucleus (Figure 2B-D). Excitatory synapse loss from cortical neurons may be a global feature in hAPP mice, or it may preferentially occur within broadly hyperactive visual network. To test this possibility, we compared synapse densities in another primary sensory cortex, the auditory cortex, which is neither hyperactive in hAPP mice nor part of the visual network. Consistent with the idea that excitatory synapse loss is preferentially associated with network hyperactivity, we did not observe synapse loss in the auditory cortex (Figure 2B-D). Interestingly, the primary visual and auditory cortexes exhibit similar hAPP burden at this stage despite differences in activity and synaptic adaptation (Figure 2E). These results suggest that

presynaptic loss is likely to be a network-related adaptation to hyperactivity rather than a causal or brain-wide alteration in amyloidosis.

VGluT2 in the visual cortex represents thalamic presynaptic inputs[90-92]. The lack of reduction in VGluT2 (thalamic synapses) density in the hyperactive primary visual cortex of hAPP mice suggests that the activity levels at the source (lateral geniculate nucleus) of presynaptic terminals rather than their target (visual cortex) may influence synapse loss. If this is the case, we expected that cortical synapses expressing VGluT1 in the non-hyperactive lateral geniculate nucleus in hAPP mice to be more reduced than VGlut2 expressing thalamic synapses. To test this, we normalized the synaptic density in individual hAPP mice to the average WT density for each synapse type. We found that the reduction in VGluT1 is higher than VGluT2 in both the visual cortex and lateral geniculate nucleus, though it did not reach statistical significance in the latter ($p = 0.08$; Figure 2F). These results indicate that presynaptic loss is not due to hyperactivity in their target brain regions.

HYPERCONNECTIVITY WITHIN THE VISUAL NETWORK AND ACROSS THE BRAIN IN AMYLOIDOSIS

Previous studies have shown hyperconnectivity in AD networks is associated with hyperactivity[9, 12, 22, 73]. To confirm if this is the case in hAPP mice, we compared functional connectivity, or correlated c-Fos$^+$ cell densities between brain regions, both within the visual network and across the brain. Brain-wide and visual network functional connectivity matrices revealed a general increase in pairwise correlation strength between brain regions with the exception of the dentate gyrus (Figure 3A). Similar results were seen for the visual network, though the cortical correlations were high even in nonpathological condition (Figure 3B). We next filtered out regional pairwise activity correlations with a p-value > 0.05 and quantified the

number of remaining connections for each node (node degree) both across the brain and within the visual network (Fig 3C-D). We observed an average of a 1.9-fold increase in node degree, both across the whole-brain network and within the visual network.

FUNCTIONAL CONNECTIVITY IN NONPATHOLOGICAL CONDITIONS ARE PREDICTIVE OF REGIONAL HYPERACTIVITY IN AMYLOIDOSIS

Multiple brain regions in ~5-month-old hAPP mice show increased c-Fos$^+$ cell density (Figure 4A). Hyperactivity may emerge independently in these brain regions or may arise through their functional connectedness with another hyperactive region. To test whether functional connectedness could contribute to hyperactivity, we next investigated whether connection strength to the primary visual cortex under nonpathological conditions is predictive of regional hyperactivity and hyperconnectivity across the brain in amyloidosis. We observed a positive brain-wide correlation between regional connection strength (measured as Pearson's r) to the primary visual cortex in the WT network and regional hyperactivity effect size in the hAPP network (Figure 4B, left). Consistently, regions with statistically significant functional connections to the primary visual cortex in WT mice displayed a higher mean effect size of hyperactivity in hAPP (Figure 4B, right). Likewise, functional connectivity strength to the primary visual cortex in the WT network trended towards positive correlation with node degrees in hAPP mice (Figure 4C, left). Consistently, regions with strong functional connections to the primary visual cortex on average formed 1.5-fold more functional connections across the brain than regions with weak or no functional connections to it (Figure 4C, right). These results indicate that functional connectivity under nonpathological conditions to a brain region that would become hyperactive in amyloid pathology partially determines their hyperactivity and hyperconnectivity phenotype in amyloidosis.

Hyperactivity of a brain region in amyloidosis may also be proportional to the number of functional connections under nonpathological conditions. Therefore, we next asked whether regions that have a higher degree of resting state functional connectivity under nonpathological conditions, both within the visual network and across the brain, are generally more at risk of becoming hyperactive in amyloidosis. To test this, we correlated the resting state node degree of each region in WT mice with the effect size of hyperactivity of the same regions in hAPP mice, both within the visual network and across all brain regions (Figure 4D). Under both conditions, we observed a significant positive correlation between node degree in the WT network and hyperactivity effect size in hAPP mice.

DISCUSSION

Here we characterize brain-wide hyperactivity at the cellular level based on immediate early gene expression and identify that visual network hyperactivity in amyloidosis stems partly from functional connectedness under nonpathological conditions. We also found that VGluT1, but not VGluT2 or VGAT expressing synapses, are reduced in both hyperactive and non-hyperactive areas of the visual network, which exhibits broad cortical hyperactivity, but not the non-hyperactive auditory cortex, which lies outside of the visual network.

Using in vivo imaging of excitatory and inhibitory postsynaptic structures in the visual cortex of hAPP mice, we recently found an increased ratio of excitatory to inhibitory synapses, indicating that structural synaptic changes favor visual cortex hyperactivity[1]. Therefore, we expected an increase in excitatory presynaptic structures as well. Surprisingly, we found that presynaptic structures harboring VGluT1 are reduced in the visual cortex of hAPP mice. This finding is consistent with a recent study showing reduced bouton density but unaltered postsynaptic spine density in the barrel cortex of the same mouse model[93]. Furthermore,

presynaptic terminals are more vulnerable at the initial stages of amyloid accumulation[94-101]. A reduction in bouton density but normal or elevated postsynaptic structures indicates that each presynaptic structure may be associated with multiple postsynaptic structures. Thus, early stages of amyloidosis could be associated with an increase in polysynaptic boutons. Polysynaptic boutons could reduce neuronal stimulus specificity and lead to memory interference. Consistently, we found that stimulus specificity is reduced in hAPP mice resulting in disrupted visual recognition memory due to interference[1]. Hippocampal-dependent memory interference is also observed in a different amyloid mouse model[102].

The reduction in excitatory presynaptic density could be due to the synaptotoxic effects of amyloid[103-108]. Inhibitory synapses have also been shown to be vulnerable to amyloid toxicity, but the results are not consistent[3, 25, 109-112]. Within the excitatory synapses, we found VGluT1 to be more vulnerable than VGluT2 in amyloid pathology. One possible cause could be the higher amyloid accumulation in VGluT1-containing boutons than in VGluT2-containing boutons[113]. An alternative possibility is that VGluT1 predominantly reflects presynaptic terminals from cortical neurons[90, 91], which are hyperactive, whereas VGluT2 in the visual cortex arises from the lateral geniculate nucleus[90-92, 114, 115], which is not hyperactive. Hyperactivity alters calcium dynamics in presynaptic structures and may lead to synaptotoxicity[5, 24, 26, 27, 116-119]. Consistent with this possibility, the auditory cortex, which does not show significant hyperactivity in hAPP mice, likewise did not show VGluT1 reduction.

A reduction in VGluT1 density in the non-hyperactive lateral geniculate nucleus and normal VGluT2 density in the hyperactive primary visual cortex suggests that hyperactivity at the source of these presynaptic terminals rather than at their target may lead to synapse loss.

Therefore, we speculate that cell-intrinsic mechanisms, such as altered presynaptic calcium dynamics[5, 24, 120-123], rather than cell-extrinsic mechanisms, such as microglia-mediated synapse removal[123-127], may be involved in the hyperactivity-associated presynaptic loss. A loss in presynaptic terminals would serve to counteract hyperactivity. Consistently, hyperactive regions tend to become more hypoactive with disease progression[22, 46, 82]. Hyperactivity-induced synapse loss is consistent with the observation that functional abnormalities precede structural abnormalities in AD[128-134].

An imbalance in excitation and inhibition triggers hyperactivity. However, there is considerable heterogeneity among brain regions in disrupting these synapse types[109-111, 135-137]. The interconnected nature of brain networks allows hyperactivity to spread to multiple brain regions without requiring local synaptic disruption. Therefore, excitatory-inhibitory disruption occurring in a hub brain region, which influences the activity of many brain structures, is likely to be more consequential in the spread of hyperactivity[28, 138-142]. In AD patients, hyperconnectivity and hyperactivity are observed in resting-state functional networks[4, 45, 128, 138, 143-145]. Furthermore, hub regions are more vulnerable to amyloid accumulation and neurodegeneration[138, 139, 143, 144, 146-150]. However, when both hyperactivity and hyperconnectivity occur, it is difficult to delineate whether increased connectivity precedes hyperactivity or vice versa, though the selective vulnerability of hub regions indicates that increased connectivity predisposes circuits to a pathological state. Once a brain region becomes hyperactive, activity-dependent amyloid production could further exacerbate hyperactivity leading to hyperconnectivity [17, 151, 152], and the vicious cycle that ensues would lead to synaptic and neurotoxicity. Consistently, we found that brain regions that are highly functionally connected under nonpathological conditions tend to become more hyperactive in amyloid

pathology, indicating that high connectivity favors the spread of hyperactivity. Functional connectivity to an impaired hub region could lead to hyperactivity in a brain region even if it lacks a direct structural connection with the hub. With multiple brain regions targeted by the same hub, coactivated activity flow could occur through multiple pathways, thus increasing the likelihood of hyperactivity. The association of higher functional connectivity with hyperactivity and subsequent accumulation of amyloid and synaptic failure indicates that randomly generated transient hyperactivity in hub regions may contribute to idiopathic AD when stabilized by the aforementioned vicious cycle.

ACKNOWLEDGEMENTS

We thank the Subramanian lab members for their help with revising this manuscript.

FUNDING

This work was supported by a grant from the National Institutes of Health (Grant No. RO1AG064067) to J.S.

CONFLICT OF INTEREST

The authors have no conflict of interest to report.

DATA AVAILABILITY STATEMENT

The data supporting the findings of this study are available on request from the corresponding author.

REFERENCES

[1] Niraula S, Doderer, J. J., Indulkar, S., Berry, K. P., Hauser, W. L., L'Esperance, O. J., Deng, J. Z., Keeter, G., Rouse, A. G., Subramanian, J. (in press) Excitation-inhibition imbalance disrupts visual familiarity in amyloid and non-pathology conditions. *Cell Rep*.

[2] Busche MA, Konnerth A (2016) Impairments of neural circuit function in Alzheimer's disease. *Philos Trans R Soc Lond B Biol Sci* **371**.

[3] Palop JJ, Chin J, Roberson ED, Wang J, Thwin MT, Bien-Ly N, Yoo J, Ho KO, Yu GQ, Kreitzer A, Finkbeiner S, Noebels JL, Mucke L (2007) Aberrant excitatory neuronal activity and compensatory remodeling of inhibitory hippocampal circuits in mouse models of Alzheimer's disease. *Neuron* **55**, 697-711.

[4] Celone KA, Calhoun VD, Dickerson BC, Atri A, Chua EF, Miller SL, DePeau K, Rentz DM, Selkoe DJ, Blacker D, Albert MS, Sperling RA (2006) Alterations in memory networks in mild cognitive impairment and Alzheimer's disease: an independent component analysis. *J Neurosci* **26**, 10222-10231.

[5] Lerdkrai C, Asavapanumas N, Brawek B, Kovalchuk Y, Mojtahedi N, Olmedillas Del Moral M, Garaschuk O (2018) Intracellular Ca(2+) stores control in vivo neuronal hyperactivity in a mouse model of Alzheimer's disease. *Proc Natl Acad Sci U S A* **115**, E1279-E1288.

[6] Bai Y, Li M, Zhou Y, Ma L, Qiao Q, Hu W, Li W, Wills ZP, Gan WB (2017) Abnormal dendritic calcium activity and synaptic depotentiation occur early in a mouse model of Alzheimer's disease. *Mol Neurodegener* **12**, 86.

[7] Busche MA, Chen X, Henning HA, Reichwald J, Staufenbiel M, Sakmann B, Konnerth A (2012) Critical role of soluble amyloid-beta for early hippocampal hyperactivity in a mouse model of Alzheimer's disease. *Proc Natl Acad Sci U S A* **109**, 8740-8745.

[8] Busche MA, Konnerth A (2015) Neuronal hyperactivity--A key defect in Alzheimer's disease? *Bioessays* **37**, 624-632.

[9] Corriveau-Lecavalier N, Rajah MN, Mellah S, Belleville S (2021) Latent patterns of task-related functional connectivity in relation to regions of hyperactivation in individuals at risk of Alzheimer's disease. *Neuroimage Clin* **30**, 102643.

[10] Kazim SF, Seo JH, Bianchi R, Larson CS, Sharma A, Wong RKS, Gorbachev KY, Pereira AC (2021) Neuronal Network Excitability in Alzheimer's Disease: The Puzzle of Similar versus Divergent Roles of Amyloid beta and Tau. *eNeuro* **8**.

[11] Targa Dias Anastacio H, Matosin N, Ooi L (2022) Neuronal hyperexcitability in Alzheimer’s disease: what are the drivers behind this aberrant phenotype? *Translational Psychiatry* **12**.

[12] Pasquini L, Rahmani F, Maleki-Balajoo S, La Joie R, Zarei M, Sorg C, Drzezga A, Tahmasian M (2019) Medial Temporal Lobe Disconnection and Hyperexcitability Across Alzheimer's Disease Stages. *J Alzheimers Dis Rep* **3**, 103-112.

[13] Ruiter M, Herstel LJ, Wierenga CJ (2020) Reduction of Dendritic Inhibition in CA1 Pyramidal Neurons in Amyloidosis Models of Early Alzheimer's Disease. *J Alzheimers Dis* **78**, 951-964.

[14] Stargardt A, Swaab DF, Bossers K (2015) Storm before the quiet: neuronal hyperactivity and Abeta in the presymptomatic stages of Alzheimer's disease. *Neurobiol Aging* **36**, 1-11.

[15] Styr B, Slutsky I (2018) Imbalance between firing homeostasis and synaptic plasticity drives early-phase Alzheimer's disease. *Nat Neurosci* **21**, 463-473.
[16] Vico Varela E, Etter G, Williams S (2019) Excitatory-inhibitory imbalance in Alzheimer's disease and therapeutic significance. *Neurobiol Dis* **127**, 605-615.
[17] Zott B, Simon MM, Hong W, Unger F, Chen-Engerer HJ, Frosch MP, Sakmann B, Walsh DM, Konnerth A (2019) A vicious cycle of beta amyloid-dependent neuronal hyperactivation. *Science* **365**, 559-565.
[18] Kazim SF, Chuang SC, Zhao W, Wong RK, Bianchi R, Iqbal K (2017) Early-Onset Network Hyperexcitability in Presymptomatic Alzheimer's Disease Transgenic Mice Is Suppressed by Passive Immunization with Anti-Human APP/Abeta Antibody and by mGluR5 Blockade. *Front Aging Neurosci* **9**, 71.
[19] Xu W, Fitzgerald S, Nixon RA, Levy E, Wilson DA (2015) Early hyperactivity in lateral entorhinal cortex is associated with elevated levels of AbetaPP metabolites in the Tg2576 mouse model of Alzheimer's disease. *Exp Neurol* **264**, 82-91.
[20] Zilberter M, Ivanov A, Ziyatdinova S, Mukhtarov M, Malkov A, Alpar A, Tortoriello G, Botting CH, Fulop L, Osypov AA, Pitkanen A, Tanila H, Harkany T, Zilberter Y (2013) Dietary energy substrates reverse early neuronal hyperactivity in a mouse model of Alzheimer's disease. *J Neurochem* **125**, 157-171.
[21] Korzhova V, Marinkovic P, Njavro JR, Goltstein PM, Sun F, Tahirovic S, Herms J, Liebscher S (2021) Long-term dynamics of aberrant neuronal activity in awake Alzheimer's disease transgenic mice. *Commun Biol* **4**, 1368.
[22] Zott B, Busche MA, Sperling RA, Konnerth A (2018) What Happens with the Circuit in Alzheimer's Disease in Mice and Humans? *Annu Rev Neurosci* **41**, 277-297.
[23] Asavapanumas N, Brawek B, Martus P, Garaschuk O (2019) Role of intracellular Ca(2+) stores for an impairment of visual processing in a mouse model of Alzheimer's disease. *Neurobiol Dis* **121**, 315-326.
[24] Verma M, Lizama BN, Chu CT (2022) Excitotoxicity, calcium and mitochondria: a triad in synaptic neurodegeneration. *Transl Neurodegener* **11**, 3.
[25] Verret L, Mann EO, Hang GB, Barth AM, Cobos I, Ho K, Devidze N, Masliah E, Kreitzer AC, Mody I, Mucke L, Palop JJ (2012) Inhibitory interneuron deficit links altered network activity and cognitive dysfunction in Alzheimer model. *Cell* **149**, 708-721.
[26] Brawek B, Garaschuk O (2014) Network-wide dysregulation of calcium homeostasis in Alzheimer's disease. *Cell Tissue Res* **357**, 427-438.
[27] Hermes M, Eichhoff G, Garaschuk O (2010) Intracellular calcium signalling in Alzheimer's disease. *J Cell Mol Med* **14**, 30-41.
[28] Maestu F, de Haan W, Busche MA, DeFelipe J (2021) Neuronal excitation/inhibition imbalance: core element of a translational perspective on Alzheimer pathophysiology. *Ageing Res Rev* **69**, 101372.
[29] Bi D, Wen L, Wu Z, Shen Y (2020) GABAergic dysfunction in excitatory and inhibitory (E/I) imbalance drives the pathogenesis of Alzheimer's disease. *Alzheimers Dement* **16**, 1312-1329.
[30] Brito-Moreira J, Paula-Lima AC, Bomfim TR, Oliveira FB, Sepulveda FJ, De Mello FG, Aguayo LG, Panizzutti R, Ferreira ST (2011) Abeta oligomers induce glutamate release from hippocampal neurons. *Curr Alzheimer Res* **8**, 552-562.

[31] Busche MA, Eichhoff G, Adelsberger H, Abramowski D, Wiederhold KH, Haass C, Staufenbiel M, Konnerth A, Garaschuk O (2008) Clusters of hyperactive neurons near amyloid plaques in a mouse model of Alzheimer's disease. *Science* **321**, 1686-1689.
[32] Findley CA, Bartke A, Hascup KN, Hascup ER (2019) Amyloid Beta-Related Alterations to Glutamate Signaling Dynamics During Alzheimer's Disease Progression. *ASN Neuro* **11**, 1759091419855541.
[33] Fogel H, Frere S, Segev O, Bharill S, Shapira I, Gazit N, O'Malley T, Slomowitz E, Berdichevsky Y, Walsh DM, Isacoff EY, Hirsch JA, Slutsky I (2014) APP homodimers transduce an amyloid-beta-mediated increase in release probability at excitatory synapses. *Cell Rep* **7**, 1560-1576.
[34] Ghatak S, Dolatabadi N, Trudler D, Zhang X, Wu Y, Mohata M, Ambasudhan R, Talantova M, Lipton SA (2019) Mechanisms of hyperexcitability in Alzheimer's disease hiPSC-derived neurons and cerebral organoids vs isogenic controls. *Elife* **8**.
[35] Hefendehl JK, LeDue J, Ko RW, Mahler J, Murphy TH, MacVicar BA (2016) Mapping synaptic glutamate transporter dysfunction in vivo to regions surrounding Abeta plaques by iGluSnFR two-photon imaging. *Nat Commun* **7**, 13441.
[36] Ovsepian SV, O'Leary VB, Zaborszky L, Ntziachristos V, Dolly JO (2019) Amyloid Plaques of Alzheimer's Disease as Hotspots of Glutamatergic Activity. *Neuroscientist* **25**, 288-297.
[37] Palop JJ, Mucke L (2010) Amyloid-beta-induced neuronal dysfunction in Alzheimer's disease: from synapses toward neural networks. *Nat Neurosci* **13**, 812-818.
[38] Paula-Lima AC, Brito-Moreira J, Ferreira ST (2013) Deregulation of excitatory neurotransmission underlying synapse failure in Alzheimer's disease. *J Neurochem* **126**, 191-202.
[39] Petrache AL, Rajulawalla A, Shi A, Wetzel A, Saito T, Saido TC, Harvey K, Ali AB (2019) Aberrant Excitatory-Inhibitory Synaptic Mechanisms in Entorhinal Cortex Microcircuits During the Pathogenesis of Alzheimer's Disease. *Cereb Cortex* **29**, 1834-1850.
[40] Sanchez PE, Zhu L, Verret L, Vossel KA, Orr AG, Cirrito JR, Devidze N, Ho K, Yu GQ, Palop JJ, Mucke L (2012) Levetiracetam suppresses neuronal network dysfunction and reverses synaptic and cognitive deficits in an Alzheimer's disease model. *Proc Natl Acad Sci U S A* **109**, E2895-2903.
[41] Scimemi A, Meabon JS, Woltjer RL, Sullivan JM, Diamond JS, Cook DG (2013) Amyloid-beta1-42 slows clearance of synaptically released glutamate by mislocalizing astrocytic GLT-1. *J Neurosci* **33**, 5312-5318.
[42] Siskova Z, Justus D, Kaneko H, Friedrichs D, Henneberg N, Beutel T, Pitsch J, Schoch S, Becker A, von der Kammer H, Remy S (2014) Dendritic structural degeneration is functionally linked to cellular hyperexcitability in a mouse model of Alzheimer's disease. *Neuron* **84**, 1023-1033.
[43] Zhang H, Liu J, Sun S, Pchitskaya E, Popugaeva E, Bezprozvanny I (2015) Calcium signaling, excitability, and synaptic plasticity defects in a mouse model of Alzheimer's disease. *J Alzheimers Dis* **45**, 561-580.
[44] Zott B, Konnerth A (2022) Impairments of glutamatergic synaptic transmission in Alzheimer's disease. *Semin Cell Dev Biol*.
[45] Sperling RA, Laviolette PS, O'Keefe K, O'Brien J, Rentz DM, Pihlajamaki M, Marshall G, Hyman BT, Selkoe DJ, Hedden T, Buckner RL, Becker JA, Johnson KA (2009)

Amyloid deposition is associated with impaired default network function in older persons without dementia. *Neuron* **63**, 178-188.
[46] Sperling RA, Dickerson BC, Pihlajamaki M, Vannini P, LaViolette PS, Vitolo OV, Hedden T, Becker JA, Rentz DM, Selkoe DJ, Johnson KA (2010) Functional alterations in memory networks in early Alzheimer's disease. *Neuromolecular Med* **12**, 27-43.
[47] Gaubert S, Raimondo F, Houot M, Corsi MC, Naccache L, Diego Sitt J, Hermann B, Oudiette D, Gagliardi G, Habert MO, Dubois B, De Vico Fallani F, Bakardjian H, Epelbaum S, Alzheimer's Disease Neuroimaging I (2019) EEG evidence of compensatory mechanisms in preclinical Alzheimer's disease. *Brain* **142**, 2096-2112.
[48] Jacobs HI, Radua J, Luckmann HC, Sack AT (2013) Meta-analysis of functional network alterations in Alzheimer's disease: toward a network biomarker. *Neurosci Biobehav Rev* **37**, 753-765.
[49] Lustig C, Snyder AZ, Bhakta M, O'Brien KC, McAvoy M, Raichle ME, Morris JC, Buckner RL (2003) Functional deactivations: change with age and dementia of the Alzheimer type. *Proc Natl Acad Sci U S A* **100**, 14504-14509.
[50] Rami L, Sala-Llonch R, Sole-Padulles C, Fortea J, Olives J, Llado A, Pena-Gomez C, Balasa M, Bosch B, Antonell A, Sanchez-Valle R, Bartres-Faz D, Molinuevo JL (2012) Distinct functional activity of the precuneus and posterior cingulate cortex during encoding in the preclinical stage of Alzheimer's disease. *J Alzheimers Dis* **31**, 517-526.
[51] Liebscher S, Keller GB, Goltstein PM, Bonhoeffer T, Hubener M (2016) Selective Persistence of Sensorimotor Mismatch Signals in Visual Cortex of Behaving Alzheimer's Disease Mice. *Curr Biol* **26**, 956-964.
[52] Elman JA, Oh H, Madison CM, Baker SL, Vogel JW, Marks SM, Crowley S, O'Neil JP, Jagust WJ (2014) Neural compensation in older people with brain amyloid-beta deposition. *Nat Neurosci* **17**, 1316-1318.
[53] Grienberger C, Rochefort NL, Adelsberger H, Henning HA, Hill DN, Reichwald J, Staufenbiel M, Konnerth A (2012) Staged decline of neuronal function in vivo in an animal model of Alzheimer's disease. *Nat Commun* **3**, 774.
[54] Oh H, Jagust WJ (2013) Frontotemporal network connectivity during memory encoding is increased with aging and disrupted by beta-amyloid. *J Neurosci* **33**, 18425-18437.
[55] Wesson DW, Borkowski AH, Landreth GE, Nixon RA, Levy E, Wilson DA (2011) Sensory network dysfunction, behavioral impairments, and their reversibility in an Alzheimer's beta-amyloidosis mouse model. *J Neurosci* **31**, 15962-15971.
[56] Deng Y, Shi L, Lei Y, Liang P, Li K, Chu WC, Wang D, Alzheimer's Disease Neuroimaging I (2016) Mapping the "What" and "Where" Visual Cortices and Their Atrophy in Alzheimer's Disease: Combined Activation Likelihood Estimation with Voxel-Based Morphometry. *Front Hum Neurosci* **10**, 333.
[57] Leow AD, Yanovsky I, Parikshak N, Hua X, Lee S, Toga AW, Jack CR, Jr., Bernstein MA, Britson PJ, Gunter JL, Ward CP, Borowski B, Shaw LM, Trojanowski JQ, Fleisher AS, Harvey D, Kornak J, Schuff N, Alexander GE, Weiner MW, Thompson PM, Alzheimer's Disease Neuroimaging I (2009) Alzheimer's disease neuroimaging initiative: a one-year follow up study using tensor-based morphometry correlating degenerative rates, biomarkers and cognition. *Neuroimage* **45**, 645-655.
[58] Reid AT, Evans AC (2013) Structural networks in Alzheimer's disease. *Eur Neuropsychopharmacol* **23**, 63-77.

[59] Weiler M, Agosta F, Canu E, Copetti M, Magnani G, Marcone A, Pagani E, Balthazar ML, Comi G, Falini A, Filippi M (2015) Following the Spreading of Brain Structural Changes in Alzheimer's Disease: A Longitudinal, Multimodal MRI Study. *J Alzheimers Dis* **47**, 995-1007.
[60] Hao J, Li K, Li K, Zhang D, Wang W, Yang Y, Yan B, Shan B, Zhou X (2005) Visual attention deficits in Alzheimer's disease: an fMRI study. *Neurosci Lett* **385**, 18-23.
[61] Balasa M, Gelpi E, Antonell A, Rey MJ, Sanchez-Valle R, Molinuevo JL, Llado A, Neurological Tissue Bank/University of Barcelona/Hospital Clinic NTBUBHCCG (2011) Clinical features and APOE genotype of pathologically proven early-onset Alzheimer disease. *Neurology* **76**, 1720-1725.
[62] Gour N, Felician O, Didic M, Koric L, Gueriot C, Chanoine V, Confort-Gouny S, Guye M, Ceccaldi M, Ranjeva JP (2014) Functional connectivity changes differ in early and late-onset Alzheimer's disease. *Hum Brain Mapp* **35**, 2978-2994.
[63] Hwang J, Kim CM, Kim JE, Oh M, Oh JS, Yoon YW, Kim JS, Lee JH, Roh JH (2021) Clinical Implications of Amyloid-Beta Accumulation in Occipital Lobes in Alzheimer's Continuum. *Brain Sci* **11**.
[64] Jacobs HI, Gronenschild EH, Evers EA, Ramakers IH, Hofman PA, Backes WH, Jolles J, Verhey FR, Van Boxtel MP (2015) Visuospatial processing in early Alzheimer's disease: a multimodal neuroimaging study. *Cortex* **64**, 394-406.
[65] Kaskie B, Storandt M (1995) Visuospatial deficit in dementia of the Alzheimer type. *Arch Neurol* **52**, 422-425.
[66] Licht EA, McMurtray AM, Saul RE, Mendez MF (2007) Cognitive differences between early- and late-onset Alzheimer's disease. *Am J Alzheimers Dis Other Demen* **22**, 218-222.
[67] Loring DW, Largen JW (1985) Neuropsychological patterns of presenile and senile dementia of the Alzheimer type. *Neuropsychologia* **23**, 351-357.
[68] Mandal PK, Joshi J, Saharan S (2012) Visuospatial perception: an emerging biomarker for Alzheimer's disease. *J Alzheimers Dis* **31 Suppl 3**, S117-135.
[69] Parasuraman R, Greenwood PM, Haxby JV, Grady CL (1992) Visuospatial attention in dementia of the Alzheimer type. *Brain* **115 (Pt 3)**, 711-733.
[70] Quental NB, Brucki SM, Bueno OF (2013) Visuospatial function in early Alzheimer's disease--the use of the Visual Object and Space Perception (VOSP) battery. *PLoS One* **8**, e68398.
[71] Sexton CE, Kalu UG, Filippini N, Mackay CE, Ebmeier KP (2011) A meta-analysis of diffusion tensor imaging in mild cognitive impairment and Alzheimer's disease. *Neurobiol Aging* **32**, 2322 e2325-2318.
[72] Tippett WJ, Sergio LE (2006) Visuomotor integration is impaired in early stage Alzheimer's disease. *Brain Res* **1102**, 92-102.
[73] Koelewijn L, Lancaster TM, Linden D, Dima DC, Routley BC, Magazzini L, Barawi K, Brindley L, Adams R, Tansey KE, Bompas A, Tales A, Bayer A, Singh K (2019) Oscillatory hyperactivity and hyperconnectivity in young APOE-varepsilon4 carriers and hypoconnectivity in Alzheimer's disease. *Elife* **8**.
[74] Keller GB, Bonhoeffer T, Hubener M (2012) Sensorimotor mismatch signals in primary visual cortex of the behaving mouse. *Neuron* **74**, 809-815.

[75] Maya-Vetencourt JF, Carucci NM, Capsoni S, Cattaneo A (2014) Amyloid plaque-independent deficit of early postnatal visual cortical plasticity in the 5XFAD transgenic model of Alzheimer's disease. *J Alzheimers Dis* **42**, 103-107.
[76] William CM, Stern MA, Pei X, Saqran L, Ramani M, Frosch MP, Hyman BT (2021) Impairment of visual cortical plasticity by amyloid-beta species. *Neurobiol Dis* **154**, 105344.
[77] William CM, Andermann ML, Goldey GJ, Roumis DK, Reid RC, Shatz CJ, Albers MW, Frosch MP, Hyman BT (2012) Synaptic plasticity defect following visual deprivation in Alzheimer's disease model transgenic mice. *J Neurosci* **32**, 8004-8011.
[78] Chiquita S, Campos EJ, Castelhano J, Ribeiro M, Sereno J, Moreira PI, Castelo-Branco M, Ambrosio AF (2019) Retinal thinning of inner sub-layers is associated with cortical atrophy in a mouse model of Alzheimer's disease: a longitudinal multimodal in vivo study. *Alzheimers Res Ther* **11**, 90.
[79] Rudinskiy N, Hawkes JM, Betensky RA, Eguchi M, Yamaguchi S, Spires-Jones TL, Hyman BT (2012) Orchestrated experience-driven Arc responses are disrupted in a mouse model of Alzheimer's disease. *Nat Neurosci* **15**, 1422-1429.
[80] Rosales Jubal E, Schwalm M, Dos Santos Guilherme M, Schuck F, Reinhardt S, Tose A, Barger Z, Roesler MK, Ruffini N, Wierczeiko A, Schmeisser MJ, Schmitt U, Endres K, Stroh A (2021) Acitretin reverses early functional network degradation in a mouse model of familial Alzheimer's disease. *Sci Rep* **11**, 6649.
[81] Papanikolaou A, Rodrigues FR, Holeniewska J, Phillips KG, Saleem AB, Solomon SG (2022) Plasticity in visual cortex is disrupted in a mouse model of tauopathy. *Commun Biol* **5**, 77.
[82] Palop JJ, Mucke L (2010) Amyloid-β–induced neuronal dysfunction in Alzheimer's disease: from synapses toward neural networks. *Nature Neuroscience* **13**, 812-818.
[83] Araya-Arriagada J, Bello F, Shivashankar G, Neira D, Durán-Aniotz C, Acosta ML, Escobar MJ, Hetz C, Chacón M, Palacios AG (2021) Retinal Ganglion Cells Functional Changes in a Mouse Model of Alzheimer’s Disease Are Linked with Neurotransmitter Alterations. *Journal of Alzheimer's Disease* **82**, S5-S18.
[84] Bass B, Upson S, Roy K, Montgomery EL, Jalonen TO, Murray IV (2015) Glycogen and amyloid-beta: key players in the shift from neuronal hyperactivity to hypoactivity observed in Alzheimer's disease? *Neural Regen Res* **10**, 1023-1025.
[85] Dickerson BC, Salat DH, Greve DN, Chua EF, Rand-Giovannetti E, Rentz DM, Bertram L, Mullin K, Tanzi RE, Blacker D, Albert MS, Sperling RA (2005) Increased hippocampal activation in mild cognitive impairment compared to normal aging and AD. *Neurology* **65**, 404-411.
[86] Harris SS, Wolf F, De Strooper B, Busche MA (2020) Tipping the Scales: Peptide-Dependent Dysregulation of Neural Circuit Dynamics in Alzheimer's Disease. *Neuron* **107**, 417-435.
[87] O'Brien JL, O'Keefe KM, LaViolette PS, DeLuca AN, Blacker D, Dickerson BC, Sperling RA (2010) Longitudinal fMRI in elderly reveals loss of hippocampal activation with clinical decline. *Neurology* **74**, 1969-1976.
[88] Ragan T, Kadiri LR, Venkataraju KU, Bahlmann K, Sutin J, Taranda J, Arganda-Carreras I, Kim Y, Seung HS, Osten P (2012) Serial two-photon tomography for automated ex vivo mouse brain imaging. *Nat Methods* **9**, 255-258.

[89] Kong H, Akakin HC, Sarma SE (2013) A generalized Laplacian of Gaussian filter for blob detection and its applications. *IEEE Trans Cybern* **43**, 1719-1733.
[90] Hackett TA, Clause AR, Takahata T, Hackett NJ, Polley DB (2016) Differential maturation of vesicular glutamate and GABA transporter expression in the mouse auditory forebrain during the first weeks of hearing. *Brain Struct Funct* **221**, 2619-2673.
[91] Varoqui H, Schafer MK, Zhu H, Weihe E, Erickson JD (2002) Identification of the differentiation-associated Na+/PI transporter as a novel vesicular glutamate transporter expressed in a distinct set of glutamatergic synapses. *J Neurosci* **22**, 142-155.
[92] Hisano S, Hoshi K, Ikeda Y, Maruyama D, Kanemoto M, Ichijo H, Kojima I, Takeda J, Nogami H (2000) Regional expression of a gene encoding a neuron-specific Na(+)-dependent inorganic phosphate cotransporter (DNPI) in the rat forebrain. *Brain Res Mol Brain Res* **83**, 34-43.
[93] Stephen TL, Tamagnini F, Piegsa J, Sung K, Harvey J, Oliver-Evans A, Murray TK, Ahmed Z, Hutton ML, Randall A, O'Neill MJ, Jackson JS (2019) Imbalance in the response of pre- and post-synaptic components to amyloidopathy. *Sci Rep* **9**, 14837.
[94] Hark TJ, Rao NR, Castillon C, Basta T, Smukowski S, Bao H, Upadhyay A, Bomba-Warczak E, Nomura T, O'Toole ET, Morgan GP, Ali L, Saito T, Guillermier C, Saido TC, Steinhauser ML, Stowell MHB, Chapman ER, Contractor A, Savas JN (2021) Pulse-Chase Proteomics of the App Knockin Mouse Models of Alzheimer's Disease Reveals that Synaptic Dysfunction Originates in Presynaptic Terminals. *Cell Syst* **12**, 141-158 e149.
[95] Barthet G, Mulle C (2020) Presynaptic failure in Alzheimer's disease. *Prog Neurobiol* **194**, 101801.
[96] de Wilde MC, Overk CR, Sijben JW, Masliah E (2016) Meta-analysis of synaptic pathology in Alzheimer's disease reveals selective molecular vesicular machinery vulnerability. *Alzheimers Dement* **12**, 633-644.
[97] He Y, Wei M, Wu Y, Qin H, Li W, Ma X, Cheng J, Ren J, Shen Y, Chen Z, Sun B, Huang FD, Shen Y, Zhou YD (2019) Amyloid beta oligomers suppress excitatory transmitter release via presynaptic depletion of phosphatidylinositol-4,5-bisphosphate. *Nat Commun* **10**, 1193.
[98] Pla V, Barranco N, Pozas E, Aguado F (2017) Amyloid-beta Impairs Vesicular Secretion in Neuronal and Astrocyte Peptidergic Transmission. *Front Mol Neurosci* **10**, 202.
[99] Russell CL, Semerdjieva S, Empson RM, Austen BM, Beesley PW, Alifragis P (2012) Amyloid-beta acts as a regulator of neurotransmitter release disrupting the interaction between synaptophysin and VAMP2. *PLoS One* **7**, e43201.
[100] Sze CI, Bi H, Kleinschmidt-DeMasters BK, Filley CM, Martin LJ (2000) Selective regional loss of exocytotic presynaptic vesicle proteins in Alzheimer's disease brains. *J Neurol Sci* **175**, 81-90.
[101] Trujillo-Estrada L, Davila JC, Sanchez-Mejias E, Sanchez-Varo R, Gomez-Arboledas A, Vizuete M, Vitorica J, Gutierrez A (2014) Early neuronal loss and axonal/presynaptic damage is associated with accelerated amyloid-beta accumulation in AbetaPP/PS1 Alzheimer's disease mice subiculum. *J Alzheimers Dis* **42**, 521-541.
[102] Poll S, Mittag M, Musacchio F, Justus LC, Giovannetti EA, Steffen J, Wagner J, Zohren L, Schoch S, Schmidt B, Jackson WS, Ehninger D, Fuhrmann M (2020) Memory trace interference impairs recall in a mouse model of Alzheimer's disease. *Nat Neurosci*.

[103] Hsieh H, Boehm J, Sato C, Iwatsubo T, Tomita T, Sisodia S, Malinow R (2006) AMPAR removal underlies Abeta-induced synaptic depression and dendritic spine loss. *Neuron* **52**, 831-843.
[104] Kamenetz F, Tomita T, Hsieh H, Seabrook G, Borchelt D, Iwatsubo T, Sisodia S, Malinow R (2003) APP processing and synaptic function. *Neuron* **37**, 925-937.
[105] Mucke L, Masliah E, Yu GQ, Mallory M, Rockenstein EM, Tatsuno G, Hu K, Kholodenko D, Johnson-Wood K, McConlogue L (2000) High-level neuronal expression of abeta 1-42 in wild-type human amyloid protein precursor transgenic mice: synaptotoxicity without plaque formation. *J Neurosci* **20**, 4050-4058.
[106] Naito Y, Tanabe Y, Lee AK, Hamel E, Takahashi H (2017) Amyloid-beta Oligomers Interact with Neurexin and Diminish Neurexin-mediated Excitatory Presynaptic Organization. *Sci Rep* **7**, 42548.
[107] Parodi J, Sepulveda FJ, Roa J, Opazo C, Inestrosa NC, Aguayo LG (2010) Beta-amyloid causes depletion of synaptic vesicles leading to neurotransmission failure. *J Biol Chem* **285**, 2506-2514.
[108] Wang Z, Jackson RJ, Hong W, Taylor WM, Corbett GT, Moreno A, Liu W, Li S, Frosch MP, Slutsky I, Young-Pearse TL, Spires-Jones TL, Walsh DM (2017) Human Brain-Derived Abeta Oligomers Bind to Synapses and Disrupt Synaptic Activity in a Manner That Requires APP. *J Neurosci* **37**, 11947-11966.
[109] Kurucu H, Colom-Cadena M, Davies C, Wilkins L, King D, Rose J, Tzioras M, Tulloch JH, Smith C, Spires-Jones TL (2022) Inhibitory synapse loss and accumulation of amyloid beta in inhibitory presynaptic terminals in Alzheimer's disease. *Eur J Neurol* **29**, 1311-1323.
[110] Mitew S, Kirkcaldie MT, Dickson TC, Vickers JC (2013) Altered synapses and gliotransmission in Alzheimer's disease and AD model mice. *Neurobiol Aging* **34**, 2341-2351.
[111] Agarwal S, Tannenberg RK, Dodd PR (2008) Reduced expression of the inhibitory synapse scaffolding protein gephyrin in Alzheimer's disease. *J Alzheimers Dis* **14**, 313-321.
[112] Hollnagel JO, Elzoheiry S, Gorgas K, Kins S, Beretta CA, Kirsch J, Kuhse J, Kann O, Kiss E (2019) Early alterations in hippocampal perisomatic GABAergic synapses and network oscillations in a mouse model of Alzheimer's disease amyloidosis. *PLoS One* **14**, e0209228.
[113] Sokolow S, Luu SH, Nandy K, Miller CA, Vinters HV, Poon WW, Gylys KH (2012) Preferential accumulation of amyloid-beta in presynaptic glutamatergic terminals (VGluT1 and VGluT2) in Alzheimer's disease cortex. *Neurobiol Dis* **45**, 381-387.
[114] Bienkowski MS, Benavidez NL, Wu K, Gou L, Becerra M, Dong HW (2019) Extrastriate connectivity of the mouse dorsal lateral geniculate thalamic nucleus. *J Comp Neurol* **527**, 1419-1442.
[115] Morimoto MM, Uchishiba E, Saleem AB (2021) Organization of feedback projections to mouse primary visual cortex. *iScience* **24**, 102450.
[116] Arbel-Ornath M, Hudry E, Boivin JR, Hashimoto T, Takeda S, Kuchibhotla KV, Hou S, Lattarulo CR, Belcher AM, Shakerdge N, Trujillo PB, Muzikansky A, Betensky RA, Hyman BT, Bacskai BJ (2017) Soluble oligomeric amyloid-beta induces calcium dyshomeostasis that precedes synapse loss in the living mouse brain. *Mol Neurodegener* **12**, 27.

[117] Calvo-Rodriguez M, Bacskai BJ (2021) Mitochondria and Calcium in Alzheimer's Disease: From Cell Signaling to Neuronal Cell Death. *Trends Neurosci* **44**, 136-151.
[118] Mattson MP, Cheng B, Davis D, Bryant K, Lieberburg I, Rydel RE (1992) beta-Amyloid peptides destabilize calcium homeostasis and render human cortical neurons vulnerable to excitotoxicity. *J Neurosci* **12**, 376-389.
[119] Supnet C, Bezprozvanny I (2010) The dysregulation of intracellular calcium in Alzheimer disease. *Cell Calcium* **47**, 183-189.
[120] Chakroborty S, Kim J, Schneider C, Jacobson C, Molgo J, Stutzmann GE (2012) Early presynaptic and postsynaptic calcium signaling abnormalities mask underlying synaptic depression in presymptomatic Alzheimer's disease mice. *J Neurosci* **32**, 8341-8353.
[121] Hermann D, Mezler M, Muller MK, Wicke K, Gross G, Draguhn A, Bruehl C, Nimmrich V (2013) Synthetic Abeta oligomers (Abeta(1-42) globulomer) modulate presynaptic calcium currents: prevention of Abeta-induced synaptic deficits by calcium channel blockers. *Eur J Pharmacol* **702**, 44-55.
[122] Tiwari SS, d'Orange M, Troakes C, Shurovi BN, Engmann O, Noble W, Hortobagyi T, Giese KP (2015) Evidence that the presynaptic vesicle protein CSPalpha is a key player in synaptic degeneration and protection in Alzheimer's disease. *Mol Brain* **8**, 6.
[123] Subramanian J, Savage JC, Tremblay ME (2020) Synaptic Loss in Alzheimer's Disease: Mechanistic Insights Provided by Two-Photon in vivo Imaging of Transgenic Mouse Models. *Front Cell Neurosci* **14**, 592607.
[124] Kettenmann H, Kirchhoff F, Verkhratsky A (2013) Microglia: new roles for the synaptic stripper. *Neuron* **77**, 10-18.
[125] Luchena C, Zuazo-Ibarra J, Alberdi E, Matute C, Capetillo-Zarate E (2018) Contribution of Neurons and Glial Cells to Complement-Mediated Synapse Removal during Development, Aging and in Alzheimer's Disease. *Mediators Inflamm* **2018**, 2530414.
[126] Rajendran L, Paolicelli RC (2018) Microglia-Mediated Synapse Loss in Alzheimer's Disease. *J Neurosci* **38**, 2911-2919.
[127] Siskova Z, Tremblay ME (2013) Microglia and synapse: interactions in health and neurodegeneration. *Neural Plast* **2013**, 425845.
[128] Bookheimer SY, Strojwas MH, Cohen MS, Saunders AM, Pericak-Vance MA, Mazziotta JC, Small GW (2000) Patterns of brain activation in people at risk for Alzheimer's disease. *N Engl J Med* **343**, 450-456.
[129] Asanad S, Felix CM, Fantini M, Harrington MG, Sadun AA, Karanjia R (2021) Retinal ganglion cell dysfunction in preclinical Alzheimer's disease: an electrophysiologic biomarker signature. *Sci Rep* **11**, 6344.
[130] Buckner RL, Snyder AZ, Shannon BJ, LaRossa G, Sachs R, Fotenos AF, Sheline YI, Klunk WE, Mathis CA, Morris JC, Mintun MA (2005) Molecular, structural, and functional characterization of Alzheimer's disease: evidence for a relationship between default activity, amyloid, and memory. *J Neurosci* **25**, 7709-7717.
[131] Damoiseaux JS (2012) Resting-state fMRI as a biomarker for Alzheimer's disease? *Alzheimers Res Ther* **4**, 8.
[132] Georgevsky D, Retsas S, Raoufi N, Shimoni O, Golzan SM (2019) A longitudinal assessment of retinal function and structure in the APP/PS1 transgenic mouse model of Alzheimer's disease. *Transl Neurodegener* **8**, 30.

[133] Kim J, Kim YH, Lee JH (2013) Hippocampus-precuneus functional connectivity as an early sign of Alzheimer's disease: a preliminary study using structural and functional magnetic resonance imaging data. *Brain Res* **1495**, 18-29.
[134] Wierenga CE, Bondi MW (2007) Use of functional magnetic resonance imaging in the early identification of Alzheimer's disease. *Neuropsychol Rev* **17**, 127-143.
[135] Berchtold NC, Coleman PD, Cribbs DH, Rogers J, Gillen DL, Cotman CW (2013) Synaptic genes are extensively downregulated across multiple brain regions in normal human aging and Alzheimer's disease. *Neurobiol Aging* **34**, 1653-1661.
[136] Kirvell SL, Esiri M, Francis PT (2006) Down-regulation of vesicular glutamate transporters precedes cell loss and pathology in Alzheimer's disease. *J Neurochem* **98**, 939-950.
[137] Tannenberg RK, Scott HL, Tannenberg AE, Dodd PR (2006) Selective loss of synaptic proteins in Alzheimer's disease: evidence for an increased severity with APOE varepsilon4. *Neurochem Int* **49**, 631-639.
[138] de Haan W, Mott K, van Straaten EC, Scheltens P, Stam CJ (2012) Activity dependent degeneration explains hub vulnerability in Alzheimer's disease. *PLoS Comput Biol* **8**, e1002582.
[139] Yu M, Sporns O, Saykin AJ (2021) The human connectome in Alzheimer disease — relationship to biomarkers and genetics. *Nature Reviews Neurology*.
[140] Crossley NA, Mechelli A, Scott J, Carletti F, Fox PT, McGuire P, Bullmore ET (2014) The hubs of the human connectome are generally implicated in the anatomy of brain disorders. *Brain* **137**, 2382-2395.
[141] Kapogiannis D, Mattson MP (2011) Disrupted energy metabolism and neuronal circuit dysfunction in cognitive impairment and Alzheimer's disease. *Lancet Neurol* **10**, 187-198.
[142] Mrdjen D, Fox EJ, Bukhari SA, Montine KS, Bendall SC, Montine TJ (2019) The basis of cellular and regional vulnerability in Alzheimer's disease. *Acta Neuropathol* **138**, 729-749.
[143] Jones DT, Knopman DS, Gunter JL, Graff-Radford J, Vemuri P, Boeve BF, Petersen RC, Weiner MW, Jack CR, Jr., Alzheimer's Disease Neuroimaging I (2016) Cascading network failure across the Alzheimer's disease spectrum. *Brain* **139**, 547-562.
[144] Schultz AP, Chhatwal JP, Hedden T, Mormino EC, Hanseeuw BJ, Sepulcre J, Huijbers W, LaPoint M, Buckley RF, Johnson KA, Sperling RA (2017) Phases of Hyperconnectivity and Hypoconnectivity in the Default Mode and Salience Networks Track with Amyloid and Tau in Clinically Normal Individuals. *J Neurosci* **37**, 4323-4331.
[145] Filippini N, MacIntosh BJ, Hough MG, Goodwin GM, Frisoni GB, Smith SM, Matthews PM, Beckmann CF, Mackay CE (2009) Distinct patterns of brain activity in young carriers of the APOE-epsilon4 allele. *Proc Natl Acad Sci U S A* **106**, 7209-7214.
[146] Jones DT, Graff-Radford J, Lowe VJ, Wiste HJ, Gunter JL, Senjem ML, Botha H, Kantarci K, Boeve BF, Knopman DS, Petersen RC, Jack CR, Jr. (2017) Tau, amyloid, and cascading network failure across the Alzheimer's disease spectrum. *Cortex* **97**, 143-159.
[147] Lehmann M, Madison CM, Ghosh PM, Seeley WW, Mormino E, Greicius MD, Gorno-Tempini ML, Kramer JH, Miller BL, Jagust WJ, Rabinovici GD (2013) Intrinsic

connectivity networks in healthy subjects explain clinical variability in Alzheimer's disease. *Proc Natl Acad Sci U S A* **110**, 11606-11611.
[148] Myers N, Pasquini L, Gottler J, Grimmer T, Koch K, Ortner M, Neitzel J, Muhlau M, Forster S, Kurz A, Forstl H, Zimmer C, Wohlschlager AM, Riedl V, Drzezga A, Sorg C (2014) Within-patient correspondence of amyloid-beta and intrinsic network connectivity in Alzheimer's disease. *Brain* **137**, 2052-2064.
[149] Palmqvist S, Scholl M, Strandberg O, Mattsson N, Stomrud E, Zetterberg H, Blennow K, Landau S, Jagust W, Hansson O (2017) Earliest accumulation of beta-amyloid occurs within the default-mode network and concurrently affects brain connectivity. *Nat Commun* **8**, 1214.
[150] Sepulcre J, Sabuncu MR, Li Q, El Fakhri G, Sperling R, Johnson KA (2017) Tau and amyloid beta proteins distinctively associate to functional network changes in the aging brain. *Alzheimers Dement* **13**, 1261-1269.
[151] Yamamoto K, Tanei ZI, Hashimoto T, Wakabayashi T, Okuno H, Naka Y, Yizhar O, Fenno LE, Fukayama M, Bito H, Cirrito JR, Holtzman DM, Deisseroth K, Iwatsubo T (2015) Chronic optogenetic activation augments abeta pathology in a mouse model of Alzheimer disease. *Cell Rep* **11**, 859-865.
[152] Cirrito JR, Yamada KA, Finn MB, Sloviter RS, Bales KR, May PC, Schoepp DD, Paul SM, Mennerick S, Holtzman DM (2005) Synaptic activity regulates interstitial fluid amyloid-beta levels in vivo. *Neuron* **48**, 913-922.

FIGURE LEGENDS

Figure 1: **Amyloidosis-associated neuronal hyperactivity emerges in cortical areas of the visual network. A)** Representative images of 24 evenly spaced landmark slices used for brain-wide c-Fos$^+$ cell density quantification. **B)** Representative image of Allen CCFv3 brain region overlay following semiautomated slice registration. **C)** Representative images of c-Fos fluorescence in the primary visual cortex of J20-hAPP mice (right) and WT littermate controls (left). The blue box is magnified below. Blue circles indicate c-Fos$^+$ cells identified by automatic cell detection. Scale bar: 1mm (top), 100µm (bottom). **D)** c-Fos$^+$ cell density across subcortical (left) and cortical (right) regions of the visual network. Data are presented as mean ± SEM, multiple *t*-tests with Benjamini-Hochberg FDR correction for all regions combined, *q-value < 0.05. n = 8 wild type (WT), 9 J20-hAPP mice.

Figure 2: **Excitatory cortical synapse loss is associated with hyperactivity A)** Representative images of synaptic immunohistochemistry labeling VGluT1 (top left), VGluT2 (top right), VGAT (bottom left), and merged channels (bottom right) in the primary visual cortex, layer 2/3. Circles indicate puncta identified by automated synapse detection. Scale bar: 5µm. **B-D)** Density of VGluT1 (B), VGluT2 (C), and VGAT (D) in primary visual cortex (VISp), dorsal lateral geniculate nucleus (LGD), and primary auditory cortex (AUD). **E)** Representative images of amyloid-β immunofluorescence with 6E10 antibody in the primary visual cortex (left) and auditory cortex (right). Scale bar: 100µm. **F)** hAPP-wild type (WT) ratio of the densities of VGluT1 and VGluT2 puncta. Data are presented as mean ± SEM, student's *t*-tests, *p-value < 0.05, # p-values between 0.05 and 0.1 displayed. n = 14 WT, 12 hAPP mice (primary visual cortex and auditory cortex). n = 13 WT, 11 hAPP mice (dorsal part of the lateral geniculate nucleus)

Figure 3: **Amyloidosis increases functional hyperconnectivity across the brain and within the visual network. (A-B)** Resting state functional connectivity matrices showing pairwise correlation (Pearson's r) of c-Fos$^+$ activity between regions across (**A)** the brain and (**B)** the visual network for wild type (WT; left) and hAPP mice (right). Region label color indicates anatomical brain area. **(C-D)** Resting state functional connections (p-value < 0.05) across (**C)** the brain and (**D)** the visual network in WT (left) and hAPP mice (right). Node color indicates anatomical brain area, node size indicates degree rank. **E)** Node degrees of selected brain regions across the brain (left) and visual network (right). Paired *t*-tests, ***p-value < 0.001, ****p-value < 0.0001. n = 8 WT, 9 hAPP mice.

Figure 4: **Brain-wide WT resting state connectivity patterns predict regional amyloidosis-induced hyperactivity and hyperconnectivity A)** Effect size (Cohen's d) of hyperactivity across the brain in hAPP mice. Dotted lines at *d* =0.8 and -0.8. **B)** Correlation of each region's functional connection strength (Pearson's r) to the visual cortex from regions across the brain in the wild type (WT) network with effect size of hyperactivity in hAPP mice (left). Linear regression with 95% confidence intervals shown. Hyperactivity effect sizes of regions that are (VIS connection$^+$) or are not (VIS connection$^-$) functionally connected (p-value < 0.05) to the visual cortex in the WT network (right). Data presented as mean ± SEM, Welch's *t*-test. **C)** Correlation between functional connection strength to the visual cortex in the WT network and node degrees in the hAPP network (left). Linear regression with 95% confidence intervals shown. Regions that are functionally connected to the visual cortex in the WT network show higher node degree in the hAPP network compared to regions that are not (right). Data presented as mean ± SEM, Welch's *t*-test. **D)** Correlation between each region's node degree in WT mice and the regional effect size of hyperactivity in hAPP mice within the visual network (left) and

across the brain (right). Linear regression with 95% confidence intervals shown. *p-value < 0.05, ***p-value < 0.001, n = 8 WT, 9 hAPP mice.

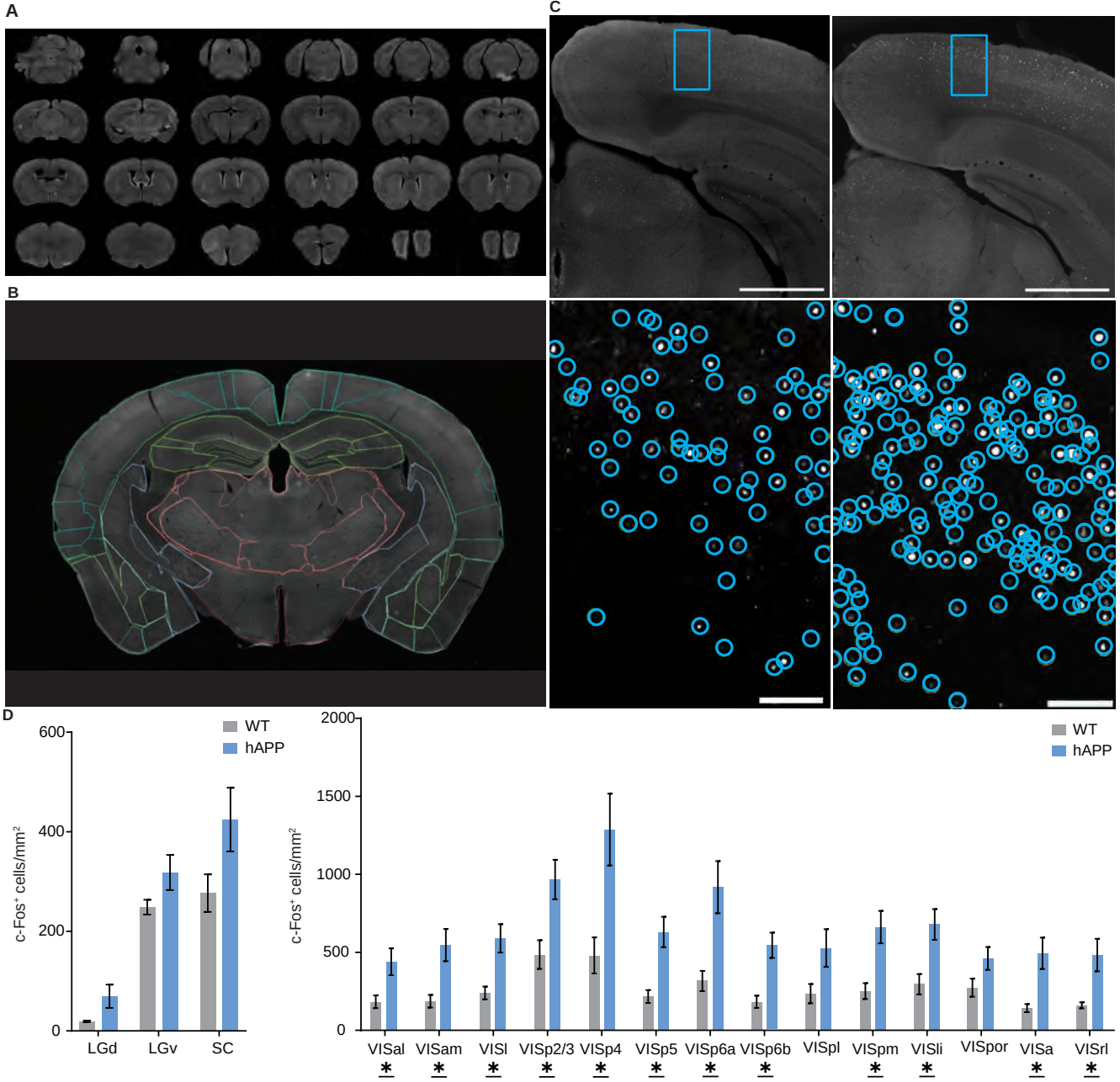
A
B
C
D
WT
hAPP
c-Fos⁺ cells/mm²
600
400
200
0
LGd
LGv
SC
2000
1500
1000
500
0
VISal
VISam
VISl
VISp2/3
VISp4
VISp5
VISp6a
VISp6b
VISpl
VISpm
VISli
VISpor
VISa
VISrl
*

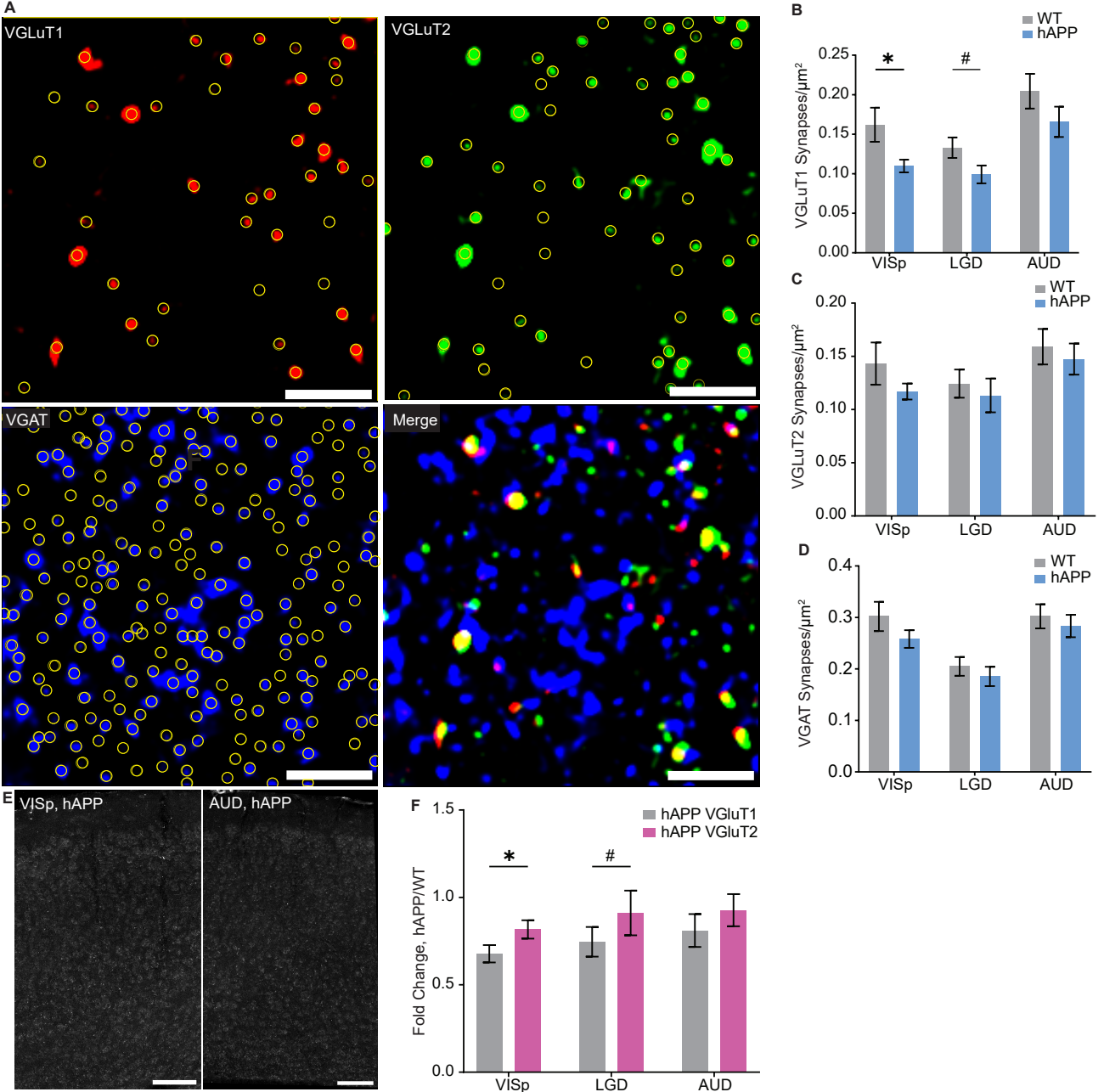
A
VGLuT1
VGLuT2
VGAT
Merge
B
WT
hAPP
VGLuT1 Synapses/µm²
0.25
0.20
0.15
0.10
0.05
0.00
*
#
VISp
LGD
AUD
C
WT
hAPP
VGLuT2 Synapses/µm²
0.20
0.15
0.10
0.05
0.00
VISp
LGD
AUD
D
WT
hAPP
VGAT Synapses/µm²
0.4
0.3
0.2
0.1
0.0
VISp
LGD
AUD
E
VISp, hAPP
AUD, hAPP
F
hAPP VGluT1
hAPP VGluT2
Fold Change, hAPP/WT
1.5
1.0
0.5
0.0
*
#
VISp
LGD
AUD

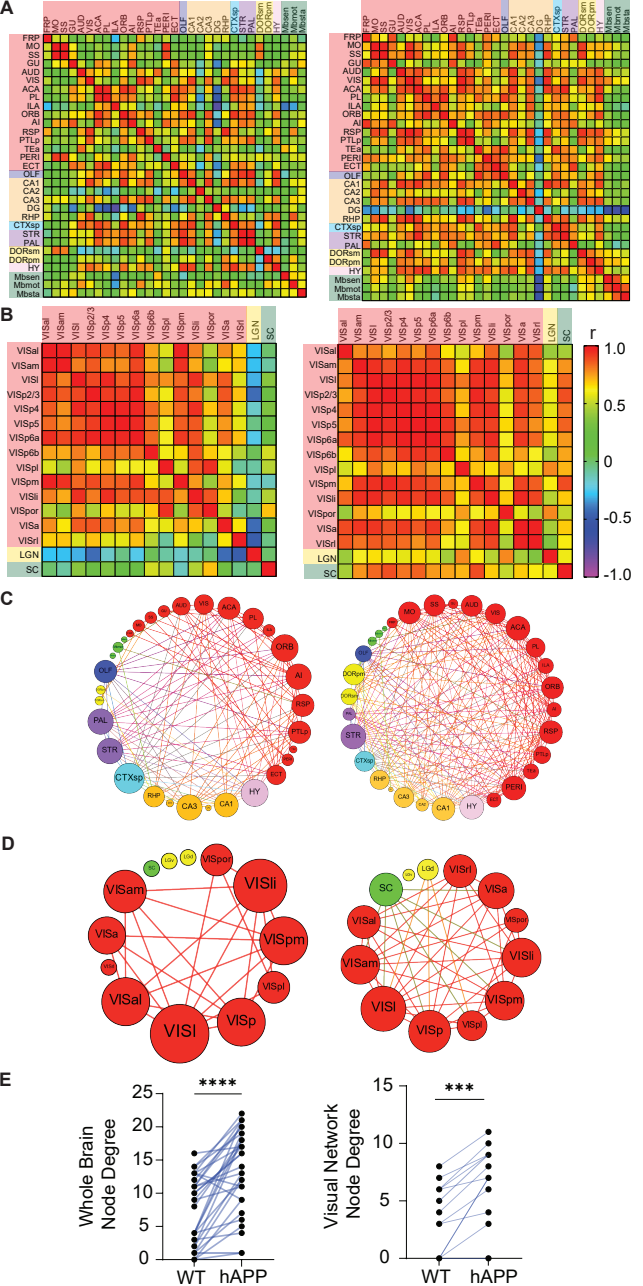
A
FRP
MO
SS
GU
AUD
VIS
ACA
PL
ILA
ORB
AI
RSP
PTLp
TEa
PERI
ECT
OLF
CA1
CA2
CA3
DG
RHP
CTXsp
STR
PAL
DORsm
DORpm
HY
Mbsen
Mbmot
Mbsta
B
VISal
VISam
VISl
VISp2/3
VISp4
VISp5
VISp6a
VISp6b
VISpl
VISpm
VISli
VISpor
VISa
VISrl
LGN
SC
r
1.0
0.5
0
-0.5
-1.0
C
D
E
****
Whole Brain Node Degree
25
20
15
10
5
0
WT
hAPP
***
Visual Network Node Degree
15
10
5
0
WT
hAPP

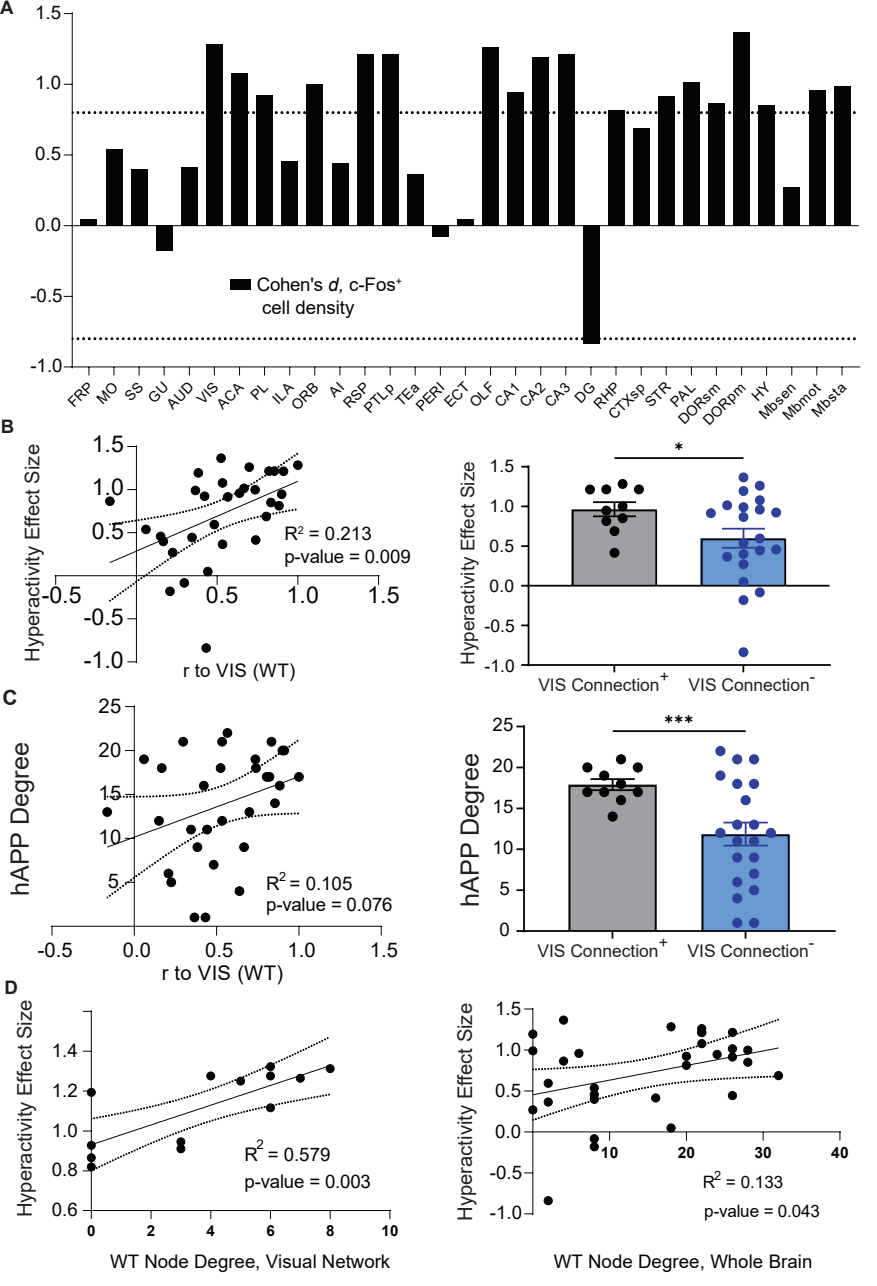
A
Cohen's d, c-Fos+ cell density
FRP MO SS GU AUD VIS ACA PL ILA ORB AI RSP PTLp TEa PERI ECT OLF CA1 CA2 CA3 DG RHP CTXsp STR PAL DORsm DORpm HY Mbsen Mbmot Mbsta
B
Hyperactivity Effect Size
r to VIS (WT)
R2 = 0.213
p-value = 0.009
VIS Connection+
VIS Connection-
C
hAPP Degree
r to VIS (WT)
R2 = 0.105
p-value = 0.076
D
WT Node Degree, Visual Network
R2 = 0.579
p-value = 0.003
WT Node Degree, Whole Brain
R2 = 0.133
p-value = 0.043